

# Microwave induced defect engineering in SiC and GaAs

Oleg Olikh<sup>1,‡</sup>, Petro Lytvyn<sup>2</sup>

<sup>1</sup>Physics Faculty, Taras Shevchenko National University of Kyiv, Kyiv 01601, Ukraine

<sup>2</sup>V. Lashkaryov Institute of Semiconductor Physics of NAS of Ukraine, Kyiv 03028, Ukraine

E-mail: olegolikh@knu.ua

**Abstract.** The influence of microwave radiation (2.45 GHz, 1.5 W/cm<sup>2</sup>, up to 80 s) on defects was studied in single crystals *n*-6H-SiC, *n*-GaAs and epi-GaAs. The capture cross-section of charge carrier has been found to change and defect complexes to be reconstructed due to the growing number of interstitial atoms in the near surface layer. The correlation between the changes in defect sub-system and deformation of the near surface layer is analyzed. The possible mechanisms of the revealed effects are discussed.

*Keywords:* microwave, defect, SiC, GaAs

Submitted to: *Semicond. Sci. Technol.*

‡ Author to whom any correspondence should be addressed.

## 1. Introduction

Microelectronics is a field of primary importance today, and the investigation of how semiconductors and their structure properties change under the action of various external factors has become one of the most important tasks in material science. A great number of theoretical and experimental researches have been aimed at revealing degradation mechanisms in microelectronic devices and developing new technologies of their production. The influence of certain factors, for example, radiation, has been studied quite well — see, for instance, [1, 2, 3]. At the same time, new agents begin to attract more attention, such as ultrasound loading (USL) [4, 5], or microwave treatment (MWT) [6, 7, 8, 9, 10, 11, 12, 13, 14, 15, 16, 17, 18, 19]. As for MWT, the superhigh frequency (SHF) electromagnetic radiation has found a wide application due to its capability to heat solid bodies [6, 7]. This approach is peculiar because of its high efficiency, capability to increase the temperature of a sample as a whole or at chosen locations with extremely high speeds of heating [6]. As a result, MWT is widely used to synthesize various compounds, semiconducting compounds including [6, 8]. However, this kind of external influence also causes the change in various characteristics of semiconductor materials and device structures. For instance, it has been found that irradiation by SHF causes the relaxation of internal stresses and modification of near surface regions in GaAs and InP structures [11, 10, 12, 13, 15, 18, 19], the leveling of surface microrelief in SiC/SiO<sub>2</sub> structures [9], redistribution of impurities [9, 16, 18] and change in charge state in the complexes [12] as well as generation of defects [16]. One of the consequences the structure-admixture ordering lead to is the decrease in the range of Schottky diode parameter spread [12, 16]. Moreover, MWT has been found to induce changes in the properties of Ti, Gd and Er films deposited on silicon carbide [17], as well as reconstruction of GaAs photoluminescence spectra [13, 15, 16], the peculiarities of the effect being dependent both on the type of dopant and crystal structure orientation of the samples. As a whole, these facts allow us to consider MWT as one of the most promising ways of modifying semiconductor devices.

On the other hand, it is of wide knowledge that the properties of semiconductor structures are determined very much by their defect subsystem. In fact, the defects in SiC and GaAs are under active investigation up to now [20, 21, 22, 23]. At the same time, the more detailed information about how MWT influences deep center parameters is practically unknown. The aim of our work is to investigate MWT impact on the parameters of deep centers located in the near surface region of *n*–6H–SiC and *n*–GaAs single crystals,

as well as on GaAs epitaxial structures by means of acoustoelectric transient spectroscopy.

## 2. Experimental details

It has been reported [11, 12, 13, 14, 15] that generally, the MWT impact on semiconductor structures depends on many factors. The main of them are the initial level of structural perfectness, conductivity, dielectric permittivity and structure topology. In order to estimate how MWT affects the defect parameters we chose different samples in view of doping degree, initial level of residual mechanical stress as well as structure. They were as follows.

- i) Single crystal *n*–6H–SiC wafers, grown by Leli method and doped with nitrogen. The samples were: 490  $\mu\text{m}$  thick plates with dimensions  $5 \times 10 \text{ mm}^2$  and carrier concentration  $(3 - 6) \times 10^{18} \text{ cm}^{-3}$  (further on SIC1 and SIC2); and 460  $\mu\text{m}$  thick wafer of the same dimensions with concentration of carriers  $(1 - 3) \times 10^{18} \text{ cm}^{-3}$  (SIC3).
- ii) GaAs single crystal plates with thickness of 300  $\mu\text{m}$ . The plates were (100) oriented, doped with tin, the concentration of electrons was  $(1.5 - 2.5) \times 10^{18} \text{ cm}^{-3}$  for sample GAS1 and  $(3 - 5) \times 10^{16} \text{ cm}^{-3}$  for sample GAS2. GAT denotation is used for wafer (111), which was doped by tellurium,  $n = (1 - 2) \times 10^{18} \text{ cm}^{-3}$ .
- iii) Epitaxial *n*–*n*<sup>+</sup> structures of GaAs which were 300  $\mu\text{m}$  thick single crystal substrates  $n = 2 \times 10^{18} \text{ cm}^{-3}$  covered with 6  $\mu\text{m}$  thick layer with carrier concentration  $3.9 \times 10^{15} \text{ cm}^{-3}$  (sample GAE1),  $3.5 \times 10^{15} \text{ cm}^{-3}$  (GAE2),  $5.0 \times 10^{15} \text{ cm}^{-3}$  (GAE3). The substrate and epitaxial layer were doped with tellurium.
- iv) Epitaxial *n*–*n*<sup>+</sup>–*n*<sup>++</sup> structures of GaAs:Te with a buffer layer. They were made from single crystal (100) substrate (300  $\mu\text{m}$ ,  $n = 2 \times 10^{18} \text{ cm}^{-3}$ ) subsequently covered with 1  $\mu\text{m}$  layer with  $n = 8 \times 10^{16} \text{ cm}^{-3}$  and 2  $\mu\text{m}$  layer with  $n = 7 \times 10^{15} \text{ cm}^{-3}$ . Two samples (GAB1 and GAB) were cut from different wafers and used in the investigation.

Epitaxial systems were produced by the gas phase epitaxy technique. The samples used in the experiment are categorized in figure 1.

MWT of the sample was carried out in free space at room temperature in the magnetron at the frequency of 2.45 GHz and specific power 1.5 W/cm<sup>2</sup>. The epitaxial structures were irradiated from the side of the epitaxial layer. The total exposition time  $t_{\text{MWT}}$  varied in the range 20 – 80 s for different samples. To avoid essential heating, the maximum single irradiation exposure time was no more than five seconds.

The parameters of deep centers, such as the efficient cross section of electron capture  $\sigma_n$  and location of the center energy level with relation to

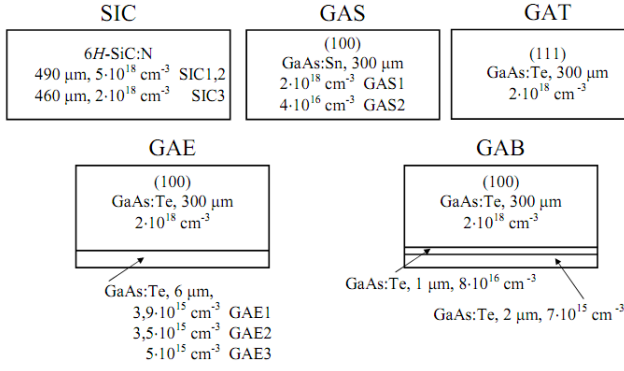


**Figure 1.** Structures for deep level investigations

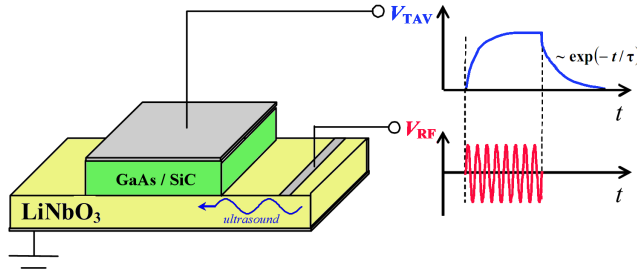


**Figure 2.** Scheme of TAV signal measurements. Time dependence of radio impulse  $V_{RF}$  of ultrasound excitation in piezoelectric plate and the resulting TAV signal  $V_{TAV}$  are shown schematically

conductivity band bottom  $E_c - E_t$  were determined before and after MWT. For this purpose, we used acoustoelectric transient spectroscopy [24, 25, 26, 27]. The method is schematically presented in figure 2. The samples were placed on the  $\text{LiNbO}_3$  piezoelectric plate in which acoustic waves were excited as impulses. After ultrasound impulse termination, the relaxation of transverse acoustoelectric voltage (TAV) takes place according to the law

$$V_{TAV}(t) = V_{TAV,0} \exp(-t/\tau). \quad (1)$$

The simple exponential dependence according to equation (1) is observed in cases when only one type of deep centers is effective in acoustoelectric interactions. For  $n$ -type semiconductor, the characteristic time of relaxation is described by equation [24, 27]

$$\tau = \frac{1}{\sigma_n v_{th,n} N_c} \exp\left(\frac{E_c - E_t}{kT}\right), \quad (2)$$

where  $v_{th,n}$  is the electron thermal velocity  $N_c$  is the densities of states in the conduction band.

The experimental measurements of the TAV relaxation at different temperatures and further approximation of the results according to equation (1) allowed us to obtain  $\tau(T)$  dependence. The  $E_c - E_t$  was determined from the slope of  $\tau$  dependence on  $(kT)^{-1}$  in semi-logarithmic scale and then, by using equation (2),  $\sigma_n$  was calculated. The measurements

were performed in the temperature range (290–350) K except GAB samples, the TAV for which was high enough to be measured only after heating to above 310 K.

For single crystal samples, before and after MWT, we also determined curvature radius  $R_{cur}$  and deformation  $\xi_{cur}$  of near surface crystallographic planes. The value of  $\xi_{cur}$  was estimated by X-ray method from the change in the angle of diffraction maximum location during sample translation [28], the curvature was measured by the profilometer DekTak 3030 Veeco Instruments.  $R_{cur}$  and  $\xi_{cur}$  were measured with a relative error no more than 2 %. For GaAs single crystals, we also analysed the distribution of structural defects over the area using the method of Borman X-ray projection topography, and estimated the distribution of dislocation densities and micro stresses from the analysis of the intensities of Friedel reflection pairs  $hkl$  and  $hk\bar{l}$ .

### 3. Results and discussion

Figure 3 presents typical temperature dependencies of  $\tau$  for the samples before and after MWT. The above data show the change not only in the curve slopes (which is directly related to the level location in the gap) but also in the absolute value of characteristic time of relaxation TAV that after MWT. The character of the MWT impact (the decrease or increase in relaxation time) depends not only on exposition time and degree of doping but also on internal structure of the samples under study. The obtained results are generalized in table 1. It is seen that in silicon carbide samples there are two deep levels, labeled ESC1 and ESC2, while in gallium arsenide, they are six (EGA1–EGA6).

### References

- [1] Kozlovskii V V, Kozlov V A and Lomasov V N 2000 *Semiconductors* **34**(2) 123–140
- [2] Schrimpf R D and Fleetwood D M 2004 *Radiation Effects and Soft Errors in Integrated Circuits and Electronic Devices* (World Scientific) ISBN 981-238-940-7
- [3] Kabiraj D and Ghosh S 2011 *J. Appl. Phys.* **109** 033701
- [4] Olikh O Y, Gorb A M, Chupryna R G and Pristay-Fenenkov O V 2018 *J. Appl. Phys.* **123** 161573
- [5] Olikh O and Pinchuk T 2006 *Tech. Phys. Lett.* **32** 517–519
- [6] Kitchen H J, Vallance S R, Kennedy J L, Tapia-Ruiz N, Carassiti L, Harrison A, Whittaker A G, Drysdale T D, Kingman S W and Gregory D H 2014 *Chem. Rev.* **114** 1170–1206
- [7] Zohm H, Kasper E, Mehringer P and Müller G 2000 *Microelectron. Eng.* **54** 247–253
- [8] Bhunia S and Bose D 1998 *J. Cryst. Growth* **186** 535–542
- [9] Bacherikov Y Y, Konakova R V, Kocherov A N, Lytvyn P M, Lytvyn O S, Okhrimenko O B and Svetlichnyi A M 2003 *Technical Physics* **48**(5) 598–601
- [10] Pashkov V, Perevoshchikov V and Skupov V 1994 *Pis'ma v zhurnal tekhnicheskoy fiziki* **20**(8) 14–18 (in Russian)

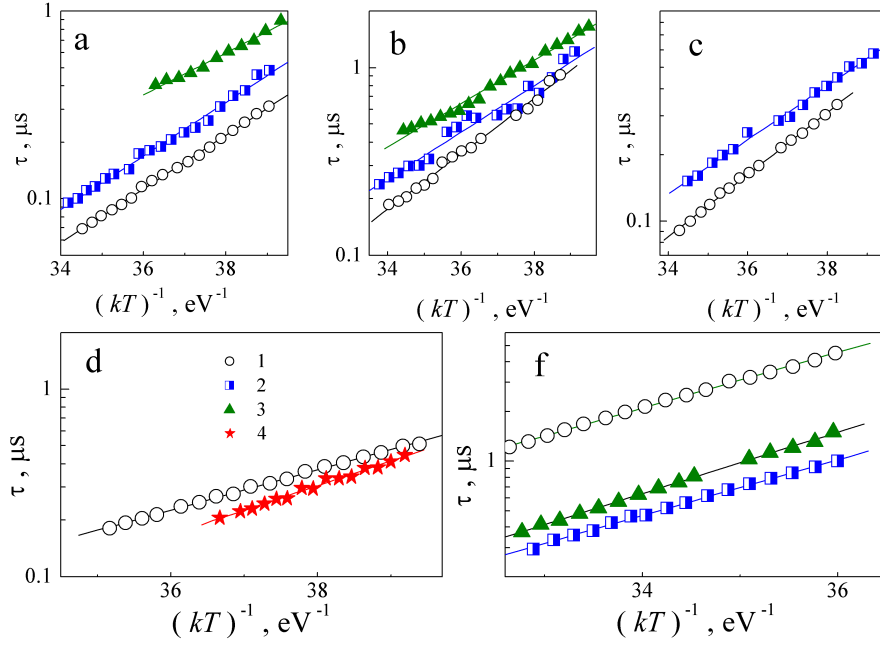


**Figure 3.** Dependences of TAV relaxation time on inverse temperature for samples SIC2 (a), SIC3 (b), GAS2 (c), GAE2 (d) and GAB1 (e) before and after MWT.  $t_{\text{MWT}}$ , s: 0 (curves 1), 20 (2), 40 (3), 60 (4)

**Table 1.** The determined defect parameters in samples  $n$ -GaAs and  $n$ -6H-SiC

Sample	$t_{\text{MWT}}$ , s	Level	$(E_c - E_t)$ , eV	$\sigma_n$ , cm <sup>2</sup> <sup>a</sup>	$R_{\text{cur}}$ , m	$\xi_{\text{cur}}$
SIC1	0	ESC1	$0.33 \pm 0.01$	$(7 \pm 4) \cdot 10^{-18}$	$\infty$	0
	20	ESC1	$0.33 \pm 0.01$	$(5 \pm 3) \cdot 10^{-19}$	170.2	$8.7 \cdot 10^{-7}$
	40	ESC2	$0.26 \pm 0.01$	$(2 \pm 1) \cdot 10^{-19}$		-
	80		weak signal			
SIC2	0	ESC1	$0.33 \pm 0.01$	$(7 \pm 4) \cdot 10^{-18}$	$> 2000$	$< 1.2 \cdot 10^{-7}$
	20	ESC1	$0.33 \pm 0.01$	$(5 \pm 3) \cdot 10^{-19}$	171.9	$1.4 \cdot 10^{-6}$
SIC3	0	ESC1	$0.34 \pm 0.02$	$(3 \pm 2) \cdot 10^{-18}$	3.8	$6.1 \cdot 10^{-5}$
	20	ESC2	$0.29 \pm 0.01$	$(5 \pm 3) \cdot 10^{-19}$	5.5	$4.2 \cdot 10^{-5}$
	40	ESC2	$0.26 \pm 0.01$	$(10 \pm 7) \cdot 10^{-20}$		-
	80	ESC2	$0.23 \pm 0.01$	$(6 \pm 4) \cdot 10^{-20}$		-
GAS1	0	EGA1	$0.32 \pm 0.02$	$(3 \pm 2) \cdot 10^{-17}$	-53.8	$-2.8 \cdot 10^{-6}$
	20	EGA1	$0.31 \pm 0.01$	$(2 \pm 1) \cdot 10^{-17}$	22.9	$6.5 \cdot 10^{-6}$
	40		weak signal			-
GAS2	0	EGA1	$0.32 \pm 0.01$	$(4 \pm 2) \cdot 10^{-17}$	17.2	$8.7 \cdot 10^{-6}$
	20	EGA2	$0.28 \pm 0.01$	$(5 \pm 2) \cdot 10^{-18}$	14.7	$1.0 \cdot 10^{-5}$
	40		weak signal			
GAT	0	EGA3	$0.49 \pm 0.02$	$(5 \pm 3) \cdot 10^{-14}$		
	20	EGA4	$0.40 \pm 0.02$	$(2 \pm 1) \cdot 10^{-15}$		
GAE1	0	EGA5	$0.24 \pm 0.01$	$(2 \pm 1) \cdot 10^{-18}$		
	60	EGA2	$0.29 \pm 0.01$	$(10 \pm 6) \cdot 10^{-18}$		
GAE2	0	EGA5	$0.25 \pm 0.01$	$(2 \pm 1) \cdot 10^{-18}$		
	60	EGA2	$0.30 \pm 0.01$	$(2 \pm 1) \cdot 10^{-17}$		
GAE3	0	EGA6	$0.43 \pm 0.01$	$(8 \pm 5) \cdot 10^{-17}$		-
	60	EGA6	$0.46 \pm 0.02$	$(7 \pm 4) \cdot 10^{-16}$		
GAB1	0	EGA4	$0.39 \pm 0.01$	$(10 \pm 7) \cdot 10^{-18}$		
	20	EGA4	$0.39 \pm 0.01$	$(4 \pm 2) \cdot 10^{-17}$		
	40	EGA6	$0.43 \pm 0.02$	$(10 \pm 6) \cdot 10^{-17}$		
GAB2	0	EGA4	$0.40 \pm 0.01$	$(10 \pm 6) \cdot 10^{-17}$		
	20	EGA4	$0.41 \pm 0.01$	$(10 \pm 6) \cdot 10^{-17}$		
	40	EGA6	$0.45 \pm 0.02$	$(4 \pm 2) \cdot 10^{-16}$		

<sup>a</sup> at  $T = 300$  K for SIC, GA, GAE and at  $T = 340$  K for GAB

- [11] Boltovets N S, Kamalov A B, Kolyadina E Y, Konakova R V, Lytvyn P M, Lytvyn O S, Matveeva L A, Milenin V V and Rengevych O E 2002 *Technical Physics Letters* **28**(2) 154–156
- [12] Milenin V, Konakova R, Statov V, Sklyarevich V, Tkhorik Y, Filatov M and Shevelev M 1994 *Pis'ma v zhurnal tekhnicheskoy fiziki* **20**(4) 32–36 (in Russian)
- [13] Belyaev A, Venger E, Ermolovich I, Konakova R, Lytvyn P, Milenin V, Prokopenko I, Svechnikov G, Soloviev E and Fedorenko L 2002 *Effect of microwave and laser radiations on the parameters of semiconductor structures* (Kyiv: Intac)
- [14] Ashkinadze B, Cohen E, Ron A, Linder E and Pfeiffer L 1996 *Solid-State Electron.* **40** 561–565 ISSN 0038-1101
- [15] Ermolovich I B, Venger E F, Konakova R V, Milenin V V, Svechnikov S V and Sheveljev M V 1998 *Proc. SPIE* **3359** 265–272
- [16] Belyayev A, Belyayev A, Yermolovich I, Komirenko S, Konakova R, Lyapin V, Milenin V, Solov'ev E and Shevelev M 1998 *Technical Physics* **43** 1445–1449
- [17] Bacherikov Y, Konakova R, Milenin V, Okhrimenko O, Svetlichnyi A and Polyakov V 2008 *Semiconductors* **42**(7) 868–872
- [18] Zayats N S, Konakova R V, Milenin V V, Milenin G V, Red'ko R A and Red'ko S N 2015 *Technical Physics* **60**(3) 432–436
- [19] Belyayev A, Sachenko A, Boltovets N, Ivanov V, Konakova R, Kudryk Y, Matveeva L, Milenin V, Novitskii S and Sheremet V 2012 *Semiconductors* **46**(4) 541–544
- [20] Davidsson J, Ivády V, Armiento R, Ohshima T, Son N T, Gali A and Abrikosov I A 2019 *Appl. Phys. Lett.* **114** 112107
- [21] Wei Y, Tarekegne A T and Ou H 2018 *J. Appl. Phys.* **124** 054901
- [22] Pellegrino C, Gagliardi A and Zimmermann C G 2020 *J. Appl. Phys.* **128** 195701
- [23] Sobolev M M, Soldatenkov F Y and Danil'chenko V G 2020 *J. Appl. Phys.* **128** 095705
- [24] Ostrovskii I V, Saiko S V and Walther H G 1998 *J. Phys. D: Appl. Phys.* **31** 2319–2325
- [25] Ostrovskii I and Olikh O 1998 *Solid State Commun.* **107** 341–343 ISSN 0038-1098
- [26] Gromashevskii V, Tatyanyenko N and Snopok B 2013 *Semiconductors* **47**(4) 579–585
- [27] Abbate A, Ostrovskii I V, Han K J, Masini G, Palma F and Das P 1995 *Semicond. Sci. Technol.* **10** 965–969
- [28] Godwod K, Nagy A T and Rek Z 1976 *Phys. Status Solidi A* **34** 705–710